

The study of Resistive Wall Mode behavior based on potential Energy analysis and feedback control in Reversed Field Pinch

Z. R. Wang¹, S. C. Guo¹, M. Baruzzo¹, T. Bolzonella¹

¹Consorzio RFX, Associazione Euratom ENEA sulla fusione, Corso Stati Uniti 4, Padova 35127, Italy

The resistive wall mode (RWM) instability and its active feedback control^[1] are important issues for different kinds of advanced fusion devices. In RFPs, RWMs as current driven modes, having their rational surfaces outside the plasma, exist as so called externally non-resonant modes (ENRMs), which have their rational surfaces located at $q < q(a) < 0$ ($q(a)$ is the safety factor at the plasma edge); and internally non-resonant modes (INRMs) with rational surfaces corresponding to $q > q(0) > 0$. In order to better understand the Resistive Wall Modes (RWMs) behavior and RWM feedback in RFP plasmas, it is essential to investigate the driving mechanisms of RWM instability and how a feedback system affects the RWMs growth rate.

In this work, we introduce a MHD cylindrical model with feedback system for studying RWM behavior and feedback control in RFP plasmas, in which the effects of the plasma pressure, compressibility, plasma inertia, longitudinal rotation and parallel viscosity (tensor) have been taken into account. The resistive wall is modeled with a finite thickness $\omega\tau_b \gg 1$ (ω is the mode frequency and τ_b is the wall penetration time scale length). Furthermore, the existing studies in toroidal geometry of RFPs have shown a weak influence of the toroidal coupling effects on the growth rate of the RWM modes^[2]. Thus a periodic cylindrical model is reasonably adopted.

I. The eigen equation and dispersion relation of RFP model including feedback control.

We introduce a cylindrical plasma with minor radius $r=a$, which is surrounded by a resistive wall at $r=b$ with thickness h and has conductivity σ . The corresponding eigenmode equation can be derived from the linearized MHD equations by assuming the perturbed displacement as $\vec{\xi}=\vec{\xi}_l(r)\exp[-i\omega+i(m\theta+kz)]$, which can be briefly written as^[3,4]

$$\frac{d}{dr}(A(\bar{\omega}) \frac{d\psi}{dr}) - C(\bar{\omega})\psi = 0 \quad (1)$$

where, $\psi = r\vec{\xi}_r$, $\bar{\omega} = \omega - \vec{k} \cdot \vec{v}_o$, the specific definition of $A(\bar{\omega})$ and $C(\bar{\omega})$ can be found in Ref.[3,4]. With respect to the RFP equilibrium parameterization, the usual “ μ - p model” is adopted, and given as $\nabla \times \vec{B}_o = \mu \vec{B}_o + (\mu_o \vec{B}_o \times \nabla p) / B_o^2$, where $\mu = 2\Theta_o [1 - (r/a)^a] / a$, and $\Theta_o = (a/R) / q(0)$. The plasma pressure profile is given by $p' = -\chi(r)(r/2\mu_o)[\mu B_o^2 / (2B_\theta) - B_z / r]^2$ which gives Suydam’s necessary condition for stability when $\chi(r) < 1$. For studying the effect of feedback control on RWMs in RFP plasmas, the feedback coil and the radial magnetic sensor are located at r_f ($r_f > b$) and r_s ($a < r_s \leq b$) respectively. Specifically, we concentrate on controlling each Fourier mode separately. Thus, for each mode, the feedback circuit is $i\omega L_f I - G_f \psi_s = R_f I$, where $\psi_s = -ir_s b_s$ is perturbed radial magnetic flux, L_f and R_f are the effective inductance and resistivity of feedback coil. The PID controller for single mode has the form $G_f = G_p + \frac{iG_i}{\omega} - i\omega G_d$, where G_p , G_i and G_d are proportional, integral and

derivative gains respectively, and defined as complex number. The boundary condition of eigenmode equation is obtained by integrating Eq.(1) over a thin layer across the plasma boundary and then taking the limit for the layer width to zero. In this way, a new boundary condition including the feedback control system is derived,

$$\frac{a^2 F_B^2}{ka} \Xi = \frac{B^2}{D+i\mu} (\bar{\omega}^2 - \omega_a^2) (\bar{\omega}^2 - i \frac{\bar{\omega} \eta_o}{\rho v_A^2} E) \frac{a}{\psi} \frac{d\psi}{dr} - 2 B_\theta^2 \\ + \frac{1}{D+i\mu} [2k B_\theta G (\bar{\omega}^2 v_A^2 - i \frac{\bar{\omega} \eta_o}{\rho} E) + i \frac{\bar{\omega} \eta_o}{\rho} \frac{B_\theta^2}{v_A^2} (\bar{\omega}^2 - \omega_a^2)] \quad (2)$$

where $\Xi = \frac{K_a' - (\frac{K_b'}{I_b'}) H_w I_a}{K_a' - (\frac{K_b'}{I_b'}) H_w I_a'} ; H_w = \frac{1}{1 + \bar{E} - \frac{i k_{0b}^2}{\omega \tau_b I_b' k^2 K_b'} \frac{1}{1 - \frac{K_s'}{K_b'} \mathbb{R}} \tanh \zeta} ; \bar{E} = \frac{I_s' / I_b' - K_s' / K_b'}{K_s' / K_b' - 1 / \mathbb{R}} ; \mathbb{R} = \text{isign}(k) \frac{\bar{G}}{\omega \tau_b (1 - \omega \tau_f)} ; \bar{G} = \frac{K_f'}{K_b} k_b^2 r_f r_s G_f ; \tau_b = \mu_o \sigma b h ; \tau_f = L_f / R_f . K_f = K_m(|k|r) \text{ and } I_f = I_m(|k|r) \text{ are the modified Bessel functions.}$

By taking $\bar{\omega} \ll \omega_a$ and ignoring the viscosity, the new dispersion relation including a movable magnetic sensor and feedback system can be expressed as:

$$-i\omega \hat{\tau}_d (1 + \bar{M}E) = \bar{M} + \text{sign}(k) \frac{\hat{\tau}_d}{\hat{\tau}_b} \frac{K_s'}{K_b} \bar{G} (1 + \bar{M}E) \quad (3)$$

where $\bar{M} = \frac{\delta W_p + \delta W_{v\infty}}{\delta W_p + \delta W_{vb}}$, $E = \bar{E} / (1 - K_b' I_a' / K_a' I_b')$, $\hat{\tau}_d = \frac{\tanh \zeta}{\zeta} \frac{K_b' I_b' k^2}{k_b^2} (1 - K_b' I_a' / K_a' I_b') \tau_b < 0$, $\hat{\tau}_b = \tau_b (1 - i\omega \tau_f)$, δW_p is

the plasma potential energy, δW_{vb} is the potential energy in vacuum region when the perfect conducting wall is located at $r=b$, and $\delta W_{v\infty}$ is also the vacuum contribution when the ideal wall is at infinity [4,5]. Note that, all the energy potential components referred in this work are normalized by $2\pi^2 R_0 \xi_a^2 / \mu_0$. The definitions of other coefficients have been given in Ref.[3-5].

When $G_f=0$, the boundary condition and dispersion relation could recover the result in Ref.[3,4].

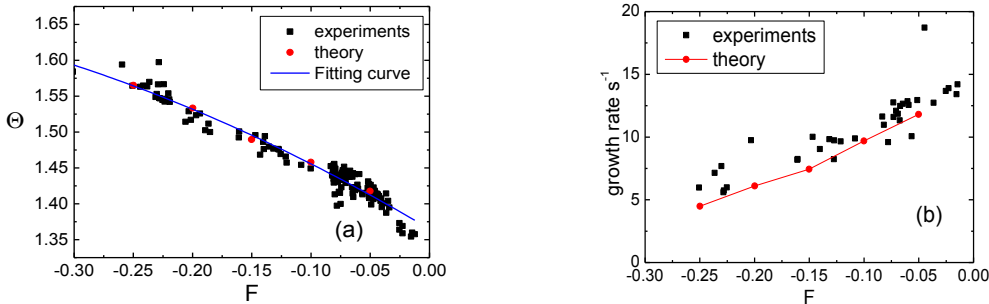


Fig.1 (a) The Θ -F curve fits to the experimental data from the database. The circle points are the selections for theoretical calculation. (b) The growth rates of $m=1, n=-5$ are plotted against F, it shows the growth rates from theory are in a good agreement with experimental measurements.

With this model, we make a comparison with experiments by assuming $\beta_p=0$ and selecting the reversal parameter F and pinch parameter Θ from the fitting curve as Fig.1(a). Figure.1(b) reports the growth rates given by the theory for $m=1 n=-5$ mode, which match the experimental growth rate well. The result implies that the μ profile adopted in RFP is reasonable and the current driven mechanism is dominant in RWM instability. Due to the sensitivity of RWM to μ profile^[4], using the measured current profile is amendatory to make a good comparison with theory.

II. Physical understanding of the role of equilibrium parameters F, Θ, β_p on RWMs' instability

When changing the value of the edge toroidal field $B_z(a)$ (which is directly related to the reversal parameter F), and keeping the current profile almost unvaried by fixing Θ_0 , the vacuum potential energy δW_{vb} is the dominant effect in the RWM instability ($|\delta W_{vb}| > |\delta W_p|$). Due to the opposite helical winding between INRM and ENRM in RFP, the variations of δW_{vb} versus F go to opposite directions between two types of the modes; this leads to the different direction of changes of the growth rates. When the pinch parameter Θ increases and parameter F remains the same, the current gradient increases; therefore, the plasma potential energy δW_p increases and the mode growth rates increase for both INRMs and ENRMs. Consequently, we clarify that the reversal parameter F mainly affects the perturbed vacuum magnetic energy, and Θ affects the plasma potential energy by changing the current profile.

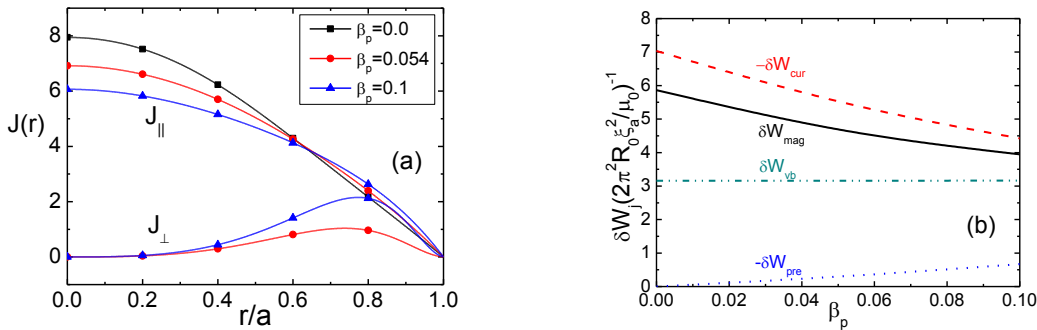


Fig.2 (a) When fixing $F=-0.05$ and $\Theta=1.45$, J_{\parallel} and J_{\perp} are plotted as the function of radial position for different β_p value, where the value of J_{\perp} is amplified 10 times. (b) The corresponding energy potential components are plotted as the function of β_p , where δW_{mag} is stabilizing term from the magnetic bending and compressibility, δW_{cur} and δW_{pre} are the current driven and pressure driven terms. δW_{vb} is the potential energy in vacuum region when the ideal wall is at $r=b$.

As for the impact of β_p , first we can further write plasma potential energy into three potential energy components $\delta W_p = \delta W_{\text{mag}} + \delta W_{\text{cur}} + \delta W_{\text{pre}}$, where δW_{mag} is stabilizing term from the magnetic bending and compressibility, δW_{cur} and δW_{pre} are the destabilizing terms from the current driven and pressure driven mechanisms. The change of β_p value may influence the shape of the current profile. Hence, the pressure and current driven mechanisms cannot vary with β_p independently. For instance, for (1,-6) mode and fixed $F=-0.05$ and $\Theta=1.45$; while raising β_p from 0 to 0.05, the mode growth rate is even decreased from 31.28 s^{-1} to 29.01 s^{-1} (about 7%). In Fig.2 (a) and (b), it shows clearly, when increasing β_p value, the diamagnetic current J_{\perp} increases on the edge of plasma, and the parallel current J_{\parallel} decreases in the plasma center and becomes less peaked simultaneously, it leads to the reduction of the current driven mechanism δW_{cur} . When β_p continuously increase up to 0.1, due to the further increasing of the pressure driven effect δW_{pre} in Fig.2 (b), the growth rate increases again, becomes 31.11 s^{-1} . Furthermore, during increasing β_p , δW_{vb} is constant. This result indicates that the variation of mode growth rate with β_p comes from the balance of δW_{cur} and δW_{pre} .

III RWM feedback control study In previous section, we introduce the feedback system into our boundary condition. The upgraded code was validated with the experimental measurements by using complex G_p phase scan^[6]. In this work, we just give an example on how the feedback

control impacts on the INRM $m=1 n=-6$ by using the real part of proportional gain G_p , and fixing $G_i, G_d=0$, more complete study of feedback control will be published in future. For this purpose, the equilibrium parameter are taken as $F=-0.05$, $\Theta=1.42$ and $\beta_p=0.02$. The magnetic sensor and feedback coil are located at $r_s/a=1.12$ (which is also the wall position), $r_f/a=1.268$, according to the RFX-mod feedback coil configuration. Without plasma rotation, when increasing the real part of G_p , the evolution of the perturbed radial magnetic field is plotted in the Fig.3(a). It indicates the feedback control just affects the perturbed vacuum magnetic field, and the perturbed magnetic field in plasma is not changed. In this case, the dispersion relation Eq. (3) can be reduced to $-i\omega\hat{\tau}_d = \bar{M} - \frac{\hat{\tau}_d}{\hat{\tau}_b} \bar{G}_p$, it implies, for stabilizing the RWM, feedback actually modifies the eddy current in the wall, which relates to the jump of perturbed magnetic field on the wall, and plasma potential energy δW_p is not affected by feedback control, the idea kink mode is still potential unstable. For the same equilibrium, when moving the magnetic sensor close to plasma, Fig.3(b) shows less G_p is required for stabilizing the $m=1, n=-6$ mode. Moreover, when the plasma rotation exists, a larger G_p should be used. For example, when $F= -0.05$, $\Theta=1.36$, $\beta_p=0.0$, for stabilizing $m=1, n=-5$ mode, without considering plasma rotation, the minimum G_p should be 0.436. When plasma velocity is 10% of poloidal Alfvén velocity on the edge of plasma (where the velocity is not in the stability windows of RFP plasmas), the minimum G_p raises up to 0.469 (increasing about 7%), whereas the perturbed b_r in plasma and plasma potential energy δW_p remain the same as those without feedback control.

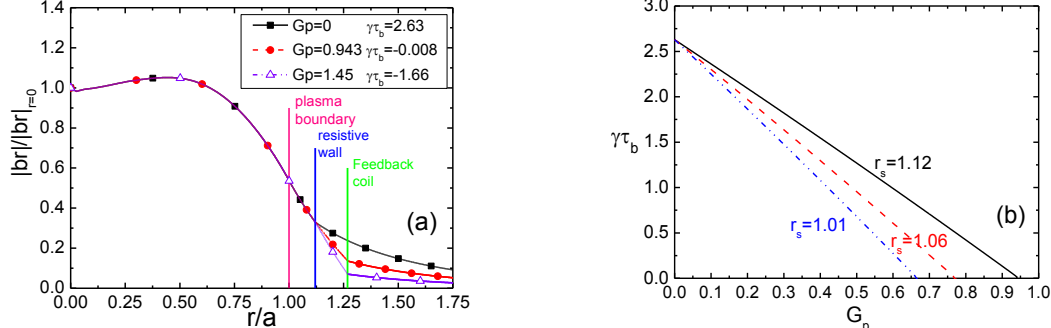


Fig 3. For $m=1 n=-6$ mode, (a) plots $|b_r|$ as the function of r for different proportional control. (b) The growth rate as the function of G_p is plotted when the sensor is located at different radial position.

Finally, due to the discrete structure of the feedback coils in reality, the magnetic sideband production from coils^[7] can lead to the modes coupling; this effect will be studied in our future work.

References

- [1] S. Ortolani and the RFX team Plasma Physics and Controlled Fusion 48, B371 (2006)
- [2] R. Paccagnella et al, NF 31,1899 (1991); F. Villone et al, PRL 100 255005 (2008)
- [3] S. C. Guo, J. P. Freidberg and R. Nachtrieb, PoP 6, 3868 (1999)
- [4] Z.R. Wang, S.C. Guo et al, PoP 17, 052501(2010)
- [5] J.P. Freidberg, "Ideal Magnetohydrodynamics" (Plemnum, New York, 1987); "Plasma Physics and Fusion Energy" (Cambridge university press, 2007)
- [6] S.C.Guo et al, 36th EPS on Plasma Physics, Sofia, Bulgaria, June 29 - July 3, 2009 [ECA Vol.33E, O-5.063 (2009)]; T. Bolzonella et al PRL 165003-1(2008)
- [7] Paccagnella et al, NF 42, 1102(2002)